

RESEARCH LETTER

10.1002/2016GL072110

Key Points:

- We provide the first observation of changing ice flow in Western Palmer Land
- Between 1992 and 2015, ice speed and discharge increased by 13% and 15 km³/yr, respectively
- The most affected glaciers are deeply grounded and flow into a thinning ice shelf, in an ocean where circumpolar deep water is shoaling

Supporting Information:

- Supporting Information S1
- Figure S1
- Figure S2
- Figure S3
- Figure S4
- Figure S5
- Table S1
- Table S2

Correspondence to:

A. E. Hogg,
a.e.hogg@leeds.ac.uk

Citation:

Hogg, A. E., et al. (2017), Increased ice flow in Western Palmer Land linked to ocean melting, *Geophys. Res. Lett.*, *44*, 4159–4167, doi:10.1002/2016GL072110.

Received 27 NOV 2016

Accepted 7 APR 2017







Accepted article online 13 APR 2017

Published online 2 MAY 2017

©2017. The Authors.

This is an open access article under the terms of the Creative Commons Attribution License, which permits use, distribution and reproduction in any medium, provided the original work is properly cited.

Increased ice flow in Western Palmer Land linked to ocean melting

Anna E. Hogg¹ , Andrew Shepherd¹ , Stephen L. Cornford^{2,3} , Kate H. Briggs¹ , Noel Gourmelen^{4,5} , Jennifer A. Graham⁶ , Ian Joughin⁷ , Jeremie Mouginot⁸ , Thomas Nagler⁹ , Antony J. Payne² , Eric Rignot^{8,10} , and Jan Wuite⁹

¹Centre for Polar Observation and Modelling, School of Earth and Environment, University of Leeds, Leeds, UK, ²Centre for Polar Observation and Modelling, School of Geographical Sciences, University of Bristol, Bristol, UK, ³Department of Geography, College of Science, Swansea University, Swansea, UK, ⁴School of Geosciences, University of Edinburgh, Edinburgh, UK, ⁵IPGS UMR 7516, Université de Strasbourg, CNRS, Strasbourg, France, ⁶Met Office Hadley Centre, Exeter, Devon, UK, ⁷Applied Physics Laboratory, University of Washington, Seattle, Washington, USA, ⁸Department of Earth System Science, University of California, Irvine, California, USA, ⁹ENVEO IT GmbH, Innsbruck, Austria, ¹⁰Jet Propulsion Laboratory, California Institute of Technology, Pasadena, California, USA

Abstract A decrease in the mass and volume of Western Palmer Land has raised the prospect that ice speed has increased in this marine-based sector of Antarctica. To assess this possibility, we measure ice velocity over 25 years using satellite imagery and an optimized modeling approach. More than 30 unnamed outlet glaciers drain the 800 km coastline of Western Palmer Land at speeds ranging from 0.5 to 2.5 m/d, interspersed with near-stagnant ice. Between 1992 and 2015, most of the outlet glaciers sped up by 0.2 to 0.3 m/d, leading to a 13% increase in ice flow and a 15 km³/yr increase in ice discharge across the sector as a whole. Speedup is greatest where glaciers are grounded more than 300 m below sea level, consistent with a loss of buttressing caused by ice shelf thinning in a region of shoaling warm circumpolar water.

1. Introduction

Over the past three decades, Antarctica's contribution to global sea level rise has been dominated by ice loss from some of its marine-based sectors [Rignot et al., 2008; Mouginot et al., 2014; Shepherd et al., 2012]. In particular, glaciers draining the Amundsen Sea sector of West Antarctica and the Antarctic Peninsula have undergone widespread retreat, acceleration, and thinning [Shepherd et al., 2002; Rignot, 2008; Shuman et al., 2011; Park et al., 2013; McMillan et al., 2014; Mouginot et al., 2014; Rignot et al., 2014; Rott et al., 2014]. These changes have been attributed to the effects of oceanic [Shepherd et al., 2003; Thomas et al., 2008; Jacobs et al., 2011; Cook et al., 2016] and atmospheric [Vaughan and Doake, 1996; Scambos et al., 2000] warming, which has eroded grounded ice and floating ice shelves at the terminus of key marine-based glaciers [Shepherd et al., 2003; Shepherd and Wingham, 2007; Pritchard et al., 2012], triggering widespread dynamical imbalance upstream [Payne et al., 2004; Joughin et al., 2012, 2014a]. Although observed changes in ice flow at the Antarctic Peninsula have been largely restricted to its northern sectors, there is evidence of recent ice shelf [Shepherd et al., 2010; Pritchard et al., 2012; Paolo et al., 2015] and grounded ice [McMillan et al., 2014; Helm et al., 2014; Wouters et al., 2015] thinning within its southerly glacier catchments, which could impact on future sea level rise.

Palmer Land contains the vast majority of the Antarctic Peninsula's ice [Fretwell et al., 2013], and its western flank is drained by glaciers along the English Coast that flow into the George VI and Stange ice shelves (Figure 1) that are predominantly grounded below sea level [Fretwell et al., 2013]. Satellite altimetry has shown that the surface of Western Palmer Land has lowered in recent years [McMillan et al., 2014; Helm et al., 2014], and this has been attributed [Wouters et al., 2015] to an episode of ice dynamic thinning contributing ~0.1 mm/yr to global sea level rise. However, because trends in the speed of English Coast glaciers have yet to be documented, this attribution remains speculative. Changes in ice sheet elevation can be caused by changes in surface mass balance or changes in ice flow. Reduced accumulation across a drainage sector leads to surface lowering over short timescales, and this is compensated over time as the ice flow readjusts (slows down) to reduced driving stress. On the other hand, if there is a relative difference in ice speedup along the glacier with greater speedup occurring downstream—which can occur through a variety of internal and external processes—the ice will be stretched and surface lowering will also ensue. Changes in ice flow can, further, be an indicator of dynamic instability, where mass loss leads to a positive

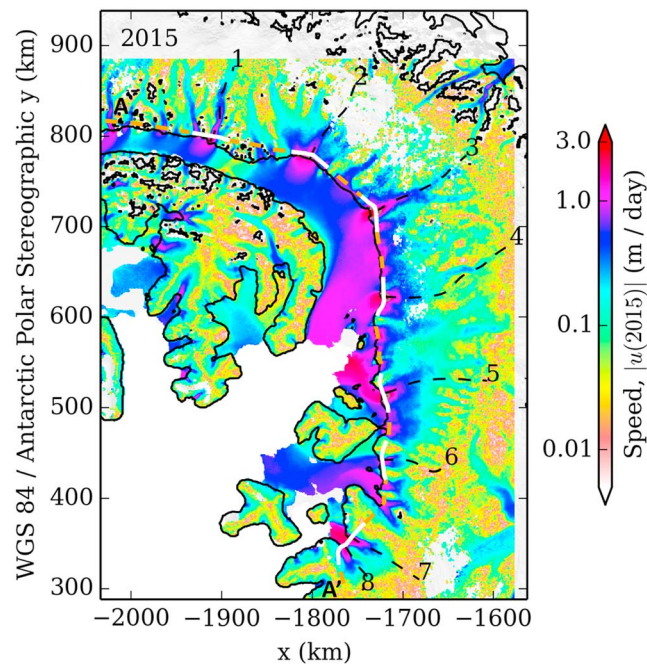


Figure 1. Ice speed (color) in Western Palmer Land at the Antarctic Peninsula measured in 2015 using repeat pass synthetic aperture radar and optical feature tracking, superimposed on a mosaic of Moderate Resolution Imaging Spectroradiometer satellite imagery (grey). Also shown are the locations of the grounding line (black line), the start (A) and end (A') of an airborne flight line where ice thickness was recorded (orange dashed line), flow lines along key outlet glaciers (black dashed line), and segments of the flow line across which ice discharge is computed (white line).

Joughin et al., 1998]. We tracked the motion of features (including speckle) in sequential SAR images acquired by the Earth Remote Sensing satellites (ERS-1 and ERS-2) in 1992, 1994, and 1996, by the Advanced Land Observation (ALOS) satellite in 2006, 2007, 2008, and 2010, and by the Sentinel-1 satellite in 2014, 2015, and 2016, and in sequential optical images acquired by the Landsat 8 satellite in 2014. We applied the interferometric technique to repeat pass SAR acquisitions acquired by the ERS-1 and ERS-2 satellites in 1995 and 1996.

Feature tracking works by measuring the displacement of features on or near to the ice surface, such as crevasses, rifts, and stable amplitude variations, across an observational period. We apply the approach to temporally sequential pairs of Single Look Complex SAR images recorded by ALOS and Sentinel-1, and to optical images recorded by the Landsat 8 Operational Land Imager. SAR image pairs were coregistered using a bilinear polynomial function constrained by precise orbital state vectors. In addition, the coregistration of ERS SAR image pairs was refined with the aid of common features on stable terrain outside areas of fast ice flow, because older mission orbits are less well constrained [*Scharroo and Visser, 1998*]. Dense networks of local, two-dimensional range and azimuth offsets were then computed from the normalized, cross correlation of real-valued intensity features present in regularly spaced SAR image patches [*Strozzi et al., 2002; Nagler et al., 2015*]. Tracked offsets with a signal-to-noise ratio lower than 4.0 were rejected. Two-dimensional offsets were computed from sequential Landsat 8 images acquired at different times [*Mouginot et al., 2014; Fahnestock et al., 2015*]. To correct the ice motion for subpixel geolocation errors in Landsat 8 images, offsets were calibrated by selecting a set of ground control points with zero velocity, and, if not available, slow motion areas [*Rignot et al., 2011a*].

We also use SAR interferometry [*Joughin et al., 1998*] to derive estimates of ice motion from “tandem” ERS-1 and ERS-2 SAR image pairs acquired 1 day apart, between March 1995 and June 1996. The technique works well on such data, because the relatively short time interval often ensures that phase coherence is preserved

feedback mechanism, such as the case of grounding line retreat on a retrograde bedrock slope [*Thomas, 1984*] in the absence of a compensating mechanism [*Gudmundsson et al., 2012*]. Because ice sheet surface lowering arising through surface mass or dynamical imbalance has opposing effects on the rate of ice flow, the origin can be established by measuring trends in ice speed. Here we measure changes in the speed of glaciers draining the English Coast of Western Palmer Land since 1992 to establish what proportion of the reported mass loss [*Wouters et al., 2015*] is due to temporal variations in ice flow.

2. Data and Methods

We measure changes in Western Palmer Land ice flow using synthetic aperture radar (SAR) and optical satellite images acquired between 1992 and 2016 (Table S1 in the supporting information). Ice velocities were computed using a combination of SAR and optical feature tracking [*Rosanova et al., 1998; Michel and Rignot, 1999*] and SAR interferometry [*Goldstein et al., 1988;*

over ice sheet surfaces. Temporally sequential SAR image pairs were again coregistered, and their phase signals were interfered on a pixel-by-pixel basis to produce differences that are related to ice motion and topography. The topographic signal was corrected using the satellite SAR imaging geometry and an elevation model [Fretwell *et al.*, 2013], and ice displacement in the SAR range direction was then computed over the image acquisition period from the remaining phase signal. We neglect atmospheric propagation delays, because they are small relative to the signal due to ice flow. Discontinuities arise in the interferometric maps of ice speed where the interferometric phase coherence falls below 0.5.

Ice velocity was computed from the feature-tracked and interferometric displacement measurements assuming that the flow is parallel to the surface, and producing a mean speed for the time interval between each image pair. The latter assumption is reasonable, as short-term fluctuations in speed are not apparent in this sector of Antarctica (Figure S4). The spatial resolution of the velocity estimates ranges from 200 to 750 m and is related to the satellite imaging geometry, the window sizes used in the feature tracking, and the interferometric multilook processing. Ice velocity estimates derived from each image pair were calibrated, geocoded, and mosaicked together [Mouginot *et al.*, 2012] on a 750 m grid to form regional maps. The estimated accuracy of individual velocity measurements within these maps ranges from 0.01 to 0.06 m/d, on average, depending on the primary data source, the processing technique, and the temporal separation of the satellite image pairs (see Figure S1).

3. Results

Our ice velocity mosaics span nine distinct epochs, and areas ranging from 810 km² in 1992 to 189,109 km² in 2015 (Table S1). Although the extent of measurements from the early 1990s is low, these data provide an important reference for key glaciers to the north of the sector. In all other years, the majority of the ice sheet margin is surveyed, though some mosaics are restricted to the coastal 50–100 km where satellite data were preferentially acquired. Mapping the uppermost reaches of the slow-moving, inland ice is persistently a challenge, due to a paucity of features. We combine velocity measurements derived from satellite images acquired within discrete temporal intervals, and generated using the same processing technique (Table S1), to produce 5 aggregated maps (Figure S1) with broad spatial coverage.

The Western Palmer Land coastline is characterized by a 300 km wide central region of ice flowing with indistinct margins between the Horne Nunataks (−71.7°S, −66.7°W) and Eklund Island (−73.2°S, −71.8°W), and by discrete glaciers separated by areas of stagnant flow elsewhere (Figure 1). Ice is transported from the inland Dyer Plateau to the Bellingshausen Sea, mainly via the George VI ice shelf into which most of the regions unnamed glaciers terminate. Of the 30+ glaciers apparent in our velocity data, 10 reach maximum speeds in excess of 1.5 m/d. However, the region of fast flow does not extend far inland, and at distances greater than 100 km from the coast few areas of ice move at speeds greater than 0.25 m/d. The region's fastest ice motion occurs at a glacier located opposite the Fauré Inlet on Alexander Island (72.6°S, 70.8°W), where speed exceeds 2.75 m/d.

Although the number and distribution of ice flow units in Western Palmer Land has remained constant throughout the 25 year study period, there have been detectable changes in speed in many locations (Figure 2). Nearly all major flow units are surveyed on at least two occasions in our data set (1995 and 2015), with several sampled in all five velocity mosaics (Figure S1). Our time series shows that the fastest flowing outlet glaciers have sped up by 0.2 to 0.3 m/d since 1992 along their central trunks, with little or no change in the slow flowing interglacial regions. Peak speeds occurred at three major ice flow units in 2010 and at one other in 2015 (Figure 2), and the average speed of ice across 28,114 km² of the sector increased from 0.31 m/d in 1995 to 0.35 m/d in 2015. The largest accelerations occurred within the central portion of Western Palmer Land where the ice flow is generally fastest, and the speedup represents a net loss of ice from the sector because it extends to the coast.

Since the satellite observations do not provide complete coverage at each epoch, we compliment them with a set of optimized (calibrated) model ice velocities (Figure S2). The optimization procedure essentially interpolates the satellite observations in space and time with the aid of an ice flow model [Cornford *et al.*, 2015], assuming spatial and temporal smoothness in the effective basal drag coefficient and the vertically averaged ice viscosity. This procedure is similar to that of Goldberg *et al.* [2015], though we seek a time-dependent (rather than time-independent) basal traction coefficient and depend upon a regularization term added to

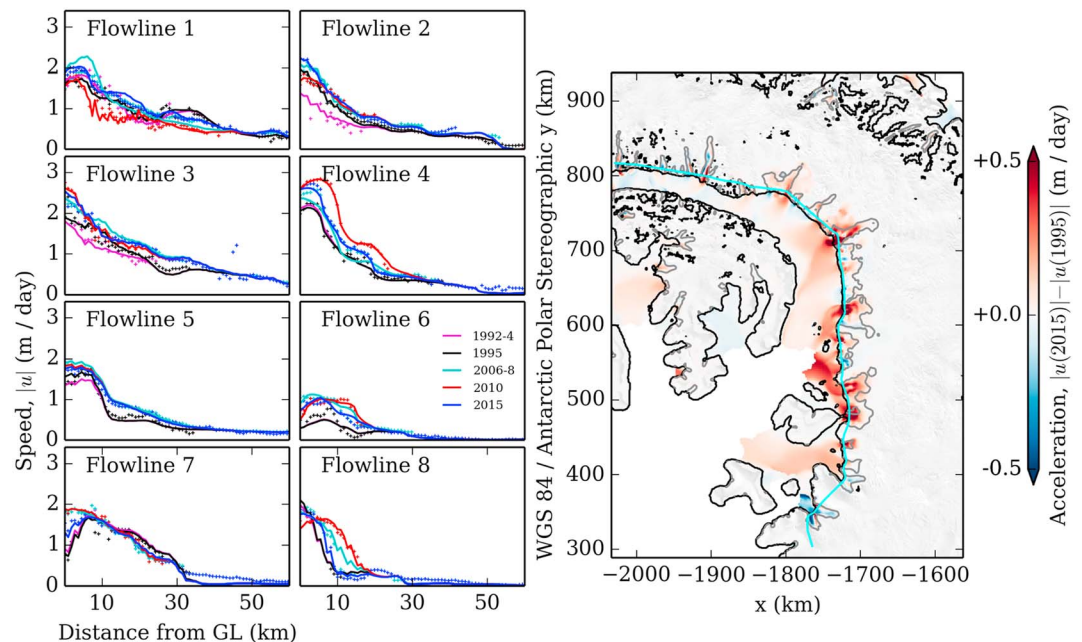


Figure 2. (left) Changes in ice speed in Western Palmer Land measured (symbols) and derived from a model optimization (lines) along glacier flow lines (see Figure 1) between 1992 and 2015, (right) and a map of ice speedup between 1995 and 2015 derived from a model optimization of the observed changes (Figures S1, S2, and S5). Also shown are the grounding line (black), the airborne flight line (cyan), and the 300 m/yr ice speed contour (grey).

the objective function to avoid abrupt temporal variations in the same fashion as abrupt spatial variations. The optimized and observed ice velocity fields agree to within 0.03 m/d, on average, in all epochs (Table S2 and Figure S3) and allow changes in flow to be investigated in areas of data omission (Figure 2).

4. Discussion

We examined changes in ice flow near to the grounding line, where ice discharge occurs, to allow a direct comparison with the estimated mass imbalance of the inland catchment [Wouters *et al.*, 2015]. This region is also where the greatest flow acceleration in response to the reported ice shelf thinning [Shepherd *et al.*, 2010; Pritchard *et al.*, 2012; Paolo *et al.*, 2015] would occur, since longitudinal stresses decay upstream [Schoof, 2007]. Although airborne records of ice thickness and elevation are relatively abundant in Western Palmer Land [Fretwell *et al.*, 2013], we focus on an 800 km coastal flight line (see Figure 1) along which precise measurements were surveyed in 2009 [Allen *et al.*, 2010]. This flight line falls, on average, within 7 km of the grounding line, as determined from satellite radar interferometry [Rignot *et al.*, 2011b]. Our velocity observations sample 86% and 83% of the flight line in 1995 and 2015, respectively (Table S1), and the thickest ice (101 and 112% of the mean thickness, respectively). Ice discharge from the sector was calculated using the observed and modeled ice speed from all five epochs, and ice thickness across a fluxgate located along the airborne flight line (Figure 1). According to the satellite measurements alone, the rate of ice discharge across the commonly observed, 83% section of this transect increased by 10% (from 80 to 88 km³/yr) between 1995 and 2015 (Figure 3). For comparison, the model optimization suggests that ice discharge across the entire gate increased by 11 km³/yr (13%) over the same period, and that the greatest proportion of ice discharge occurs through the central region (flow unit 3) of Western Palmer Land (Table 1). Furthermore, our model suggests that ice discharge across the gate peaked at 106 km³/yr in 2010 and has dropped since then to 100 km³/yr.

A number of studies [Helm *et al.*, 2014; McMillan *et al.*, 2014; Wouters *et al.*, 2015] have documented a recent lowering of the grounded ice sheet surface in this sector of Antarctica, with peak rates in the range 2 to 3 m/yr near to the grounding line, leading to an estimated [Wouters *et al.*, 2015] 31 to 43 km³/yr thinning of the inland ice between 2010 and 2014. Our results (Table 1) confirm that part of this thinning is associated

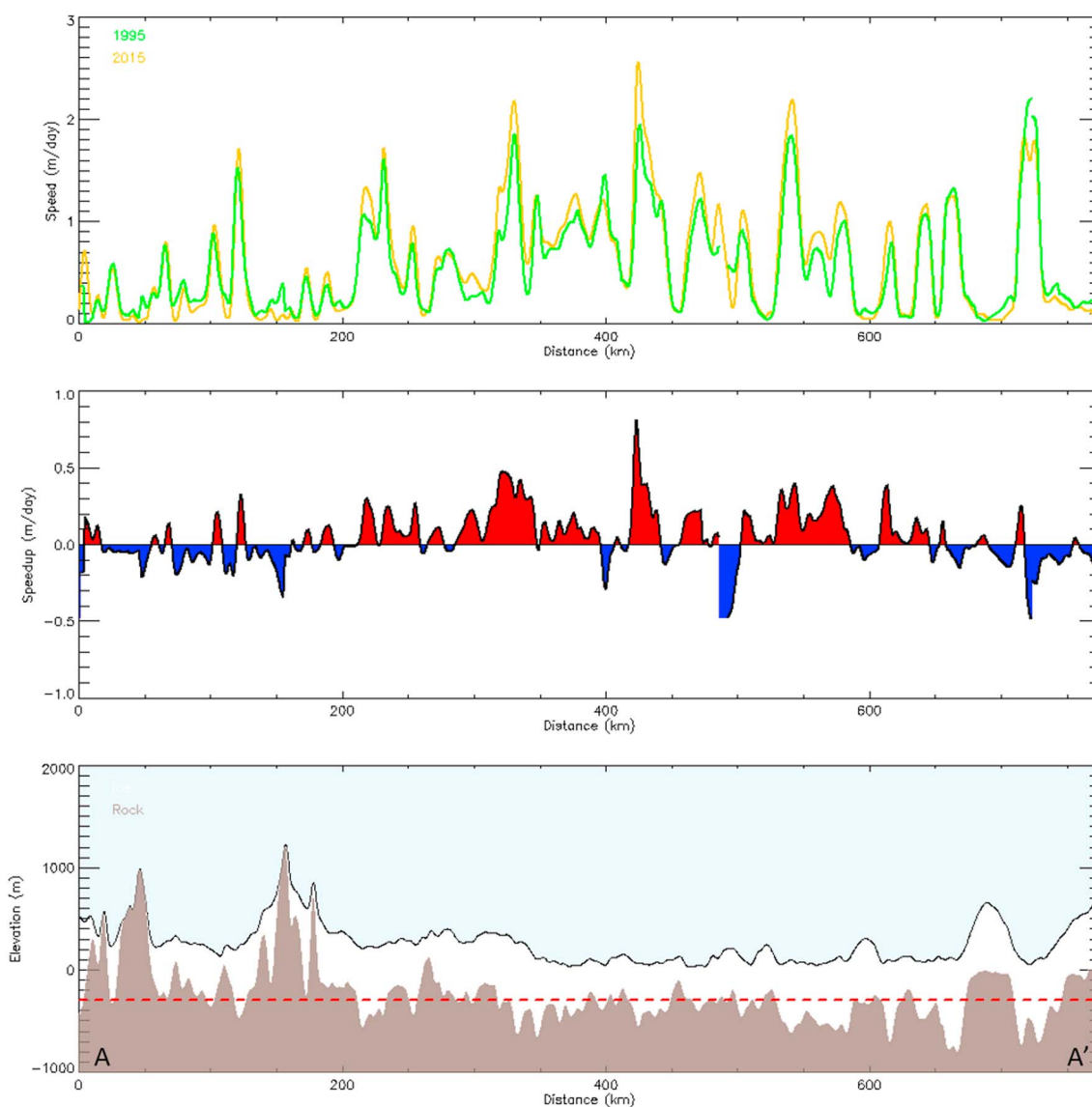


Figure 3. (top) Ice speed in 1995 (green) and 2015 (amber), (middle) speedup between 1995 and 2015, (bottom) and geometry (c) measured along a southerly airborne flight line of the English Coast, Western Palmer Land (see Figure 1). Red dashed line (Figure 3, bottom) highlights the -300 m bedrock elevation threshold, and the start (A) and end (A') location of the flight line are also annotated.

Table 1. Ice Discharge Across 40 km Wide Segments of a Southerly Airborne Flight Line of the English Coast, Western Palmer Land (See Figure 1) Computed From Model Optimized Ice Velocity Data^a

Year	Unit 1 (km ³ /yr)	Unit 2 (km ³ /yr)	Unit 3 (km ³ /yr)	Unit 4 (km ³ /yr)	Unit 5 (km ³ /yr)	Unit 6 (km ³ /yr)	Unit 7 (km ³ /yr)	Unit 8 (km ³ /yr)	Rest (km ³ /yr)	All (km ³ /yr)
1992–6	4.0	6.2	9.4	8.6	6.1	1.5	9.1	9.6	29.6	84.5
1995–6	3.7	8.5	10.3	8.5	6.9	1.5	9.4	9.9	29.6	88.3
2006–8	4.6	9.9	12.9	10.0	8.4	2.7	8.9	9.3	35.3	102.0
2010	4.4	10.0	14.9	11.5	8.7	2.3	8.2	8.5	37.7	106.4
2014–16	4.0	9.4	13.4	10.6	8.3	2.3	8.2	8.5	35.1	99.7

^aLocations and epochs where 25% or less of the segments were constrained with observations are italicized.

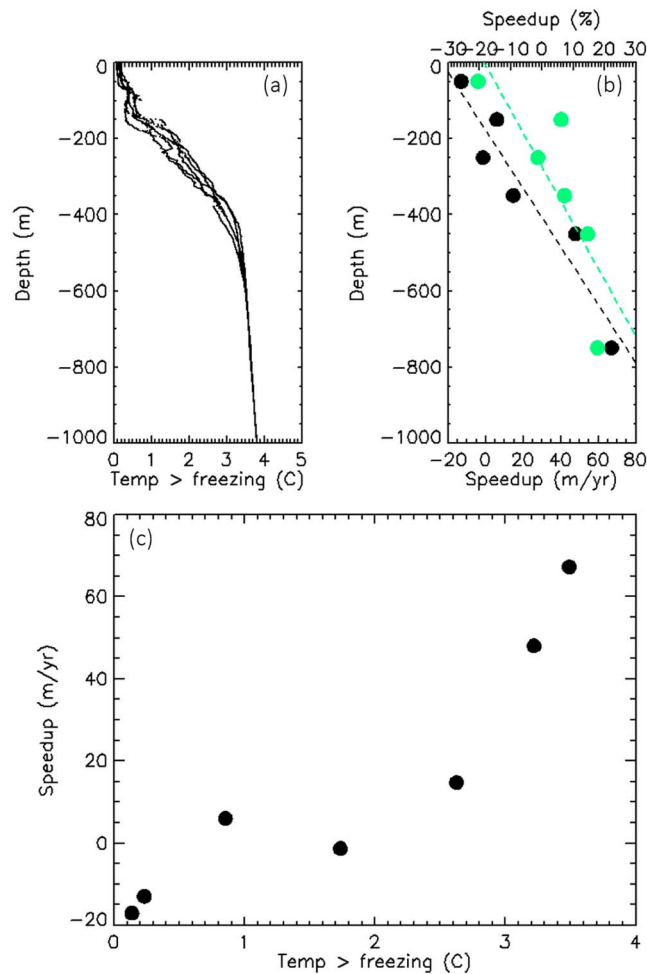


Figure 4. (a) Bellingshausen Sea ocean temperature depth profiles. (b) Average variation in absolute (black dots) and relative (green dots) ice speedup along a southerly airborne flight line of the English Coast, Western Palmer Land (see Figure 1) according to the depth at which the ice is grounded below sea level in 100 m elevation bands. (c) Average variation in ice speedup along the southerly airborne flight line shown against ocean temperature at the corresponding depth below present-day sea level.

theoretical arguments [Schoof, 2007] relating changes in the depth, speed, and instantaneous acceleration of ice flowing across the grounding line in response to changes in ocean forcing or ice stream rheology (either englacial or at the bed) (Figure S5). Satellite altimetry has shown [Shepherd et al., 2010; Paolo et al., 2015] that the George VI ice shelf (into which English Coast glaciers flow) has thinned at rates of between 0.8 and 1.0 m/yr since the early 1990s, providing evidence against a (solely) rheological cause for the speedup, which (alone) would lead to ice shelf thickening. This leaves ocean-driven melting, leading to both ice shelf thinning and ice stream speedup, as the remaining possible source of the imbalance.

We examined the evidence for the surrounding ocean being the source of the increased ice flow. Warm circumpolar deep water (CDW) is present within the Bellingshausen Sea [Holland et al., 2010] and floods, periodically, through bathymetric depressions onto the continental shelf [Moffat et al., 2009] and into the ocean cavity beneath George VI ice shelf [Potter and Paren, 1985; Talbot, 1988; Jenkins and Jacobs, 2008]. This water is more than 3°C warmer than the local freezing temperature and has been recorded at depths below 200 to 300 m in the wider Bellingshausen Sea [Hofmann et al., 2009; Kimura et al., 2015] and at 340 m at the base of George VI ice shelf [Kimura et al., 2015]. Model simulations [e.g., Holland et al., 2010] suggests that it flushes much of the subshef cavity, where it is estimated [Kimura et al., 2015] to generate

with increased ice flow. However, the rate of ice discharge from the sector during the 2010s was only 11 to 15 km³/yr greater than during the 1990s, and so increased flow is only responsible for a small fraction (35%) of the inland thinning. The remainder (65%) is not associated with dynamical thinning of the inland ice. A possible explanation for the discrepancy lies in the impact of short-term snowfall fluctuations, which are an important and a common factor in estimates of ice sheet mass change derived from both satellite altimetry and satellite gravimetry and which are notoriously difficult to characterize in areas of rugged terrain and high accumulation such as the Antarctic Peninsula [Wouters et al., 2013].

To investigate the physical process responsible for the increased ice discharge from Western Palmer Land, we examined the spatial pattern of glacier speedup, which is highly localized (Figure 2). Although lower accumulation may have led to some of the inland deflation, it can be eliminated as a cause of the velocity change because it would reduce the total driving stress over time and, in turn, slow the ice. We must therefore turn to other parts of the force balance for an explanation. The greatest speedup has occurred on glaciers with the fastest initial speed (Figures 1, 2, and S5), and these typically flow through deep bedrock troughs (Figure 3). This behavior is in line with

melting in the range 0.1 to 1.3 m/yr at the base of George VI ice shelf—consistent with the reported ice shelf thinning [Shepherd *et al.*, 2010; Pritchard *et al.*, 2012; Paolo *et al.*, 2015]. Long-term temperature records [Schmidtke *et al.*, 2014] show that the distribution of CDW across the region has shoaled, leading to a 0.1° to 0.3°C decade⁻¹ warming since 1979—evidence that the forcing may have increased over time. Despite the regional ice being grounded well below sea level along the majority of the English Coast (Figure 3), significant speedup has only occurred at glaciers that flow along bedrock troughs that are deeper than 300 m below present-day sea level (Figure 4). However, this pattern corresponds to the depth at which CDW is present (Figure 4c), providing a link between the surrounding ocean and the observed change in ice flow. We hypothesize that ocean-driven melting may have triggered modest dynamical thinning of ice in Western Palmer Land—a process that has led to widespread drawdown of inland ice in other sectors of Antarctica [Shepherd *et al.*, 2002; Rignot *et al.*, 2008; Payne *et al.*, 2004; Joughin *et al.*, 2014a].

5. Conclusions

We provide the first observational evidence that dynamic thinning of ice is occurring at glaciers along the English Coast in Western Palmer Land. Using satellite observations, we show that the rate of ice flow across the sector as a whole has increased by 13% (from 0.31 to 0.35 m/d) since 1995 and, with the aid of an optimized ice sheet model, we show that the rate of ice discharge across a gate near to the grounding line has increased by 13% (from 88.3 to 99.7 km³/yr) over the same period. Though significant, the dynamical imbalance is responsible for only a small proportion (35%) of the deflation that has occurred inland [Helm *et al.*, 2014; McMillan *et al.*, 2014; Wouters *et al.*, 2015]. The pattern of increased ice flow coincides with the distribution of glaciers that are grounded more than 300 m below sea level, which corresponds to the depth at which warm circumpolar deep water resides within the neighboring ocean [Hofmann *et al.*, 2009; Kimura *et al.*, 2015]. A large fraction of Western Palmer Land is grounded well below sea level, and so there is a prospect that the ice dynamical imbalance could lead to further draw down of ice from the interior over time—as it has occurred in other sectors of Antarctica [Shepherd *et al.*, 2002; Rignot, 2008; Payne *et al.*, 2004; Joughin *et al.*, 2014a]. With enough ice to raise global sea level by over 20 cm [Fretwell *et al.*, 2013], the future evolution of dynamical imbalance in Western Palmer Land should be accounted for in projections of global sea level rise.

Acknowledgments

We thank Adrian Jenkins for providing ocean temperature observations. This work was led by the NERC Centre for Polar Observation and Modelling, supported by the Natural Environment Research Council (cpom300001), with the support of a grant (4000107503/13/I-BG) from the European Space Agency's support to Science Element program and an independent research fellowship (4000112797/15/I-SBo) jointly funded by the European Space Agency, the University of Leeds, and the British Antarctic Survey. The authors gratefully acknowledge the ESA, the National Aeronautics and Space Administration, and the Japan Aerospace Exploration Agency for the use of ERS-1 and ERS-2 (C1P9925), Sentinel-1, Landsat 8, and ALOS PALSAR data, respectively.

References

- Allen, C., C. Leuschen, P. Gogineni, F. Rodriguez-Morales, J. Paden (2010), updated 2015, *IceBridge MCoRDS L2 Ice Thickness*, [IRMC2_20091103_02], NASA Natl. Snow and Ice Data Cent., Distributed Active Archive Center, Boulder, Colo., doi:10.5067/GDQ0CUCVTE2Q.
- Cook, A. J., P. R. Holland, M. P. Meredith, T. Murray, A. Luckman, and D. G. Vaughan (2016), Ocean forcing of glacier retreat in the western Antarctic Peninsula, *Science*, 353(6296), 283–286, doi:10.1126/science.aae0017.
- Cornford, S. L., et al. (2015), Century-scale simulations of the response of the West Antarctic Ice Sheet to a warming climate, *Cryosphere*, 9, 1579–1600, doi:10.5194/tc-9-1579-2015.
- Fretwell, P., et al. (2013), Bedmap2: Improved ice bed, surface and thickness datasets for Antarctica, *Cryosphere*, 7, 375–393, doi:10.5194/tc-7-375-2013.
- Fahnestock, M., T. Scambos, T. Moon, A. Gardner, T. Haran, and M. Klinger (2015), Rapid large-area mapping of ice flow using Landsat 8, *Remote Sens. Environ.*, 185, 84–94, doi:10.1016/j.rse.2015.11.023.
- Goldberg, D. N., P. Heimbach, I. Joughin, and B. Smith (2015), Committed retreat of Smith, Pope, and Kohler Glaciers over the next 30 years inferred by transient model calibration, *Cryosphere*, 9, 2429–2446, doi:10.5194/tc-9-2429-2015.
- Goldstein, R. M., H. A. Zebker, and C. L. Werner (1988), Satellite radar interferometry: Two-dimensional phase unwrapping, *Radio Sci.*, 23(4), 713–720, doi:10.1029/RS023i004p00713.
- Gudmundsson, G. H., J. Krug, G. Durand, L. Favier, and O. Gagliardini (2012), The stability of grounding lines on retrograde slopes, *Cryosphere*, 6, 1497–1505, doi:10.5194/tc-6-1497-2012.
- Helm, V., A. Humbart, and H. Miller (2014), Elevation and elevation change of Greenland and Antarctica derived from CryoSat-2, *Cryosphere*, 8, 1539–1559, doi:10.5194/tc-8-1539-2014.
- Hofmann, E. E., D. P. Costa, K. Daly, M. S. Dinniman, J. M. Klinck, M. Marrari, L. Padman, and A. Piñones (2009), Results from the U.S. Southern Ocean GLOBEC synthesis studies, *GLOBEC Int. Newsl.*, 15, 43–48.
- Holland, P. R., A. Jenkins, and D. M. Holland (2010), Ice and ocean processes in the Bellingshausen Sea, Antarctica, *J. Geophys. Res.*, 115, C05020, doi:10.1029/2008JC005219.
- Jacobs, S. S., A. Jenkins, C. F. Giulivi, and P. Dutrieux (2011), Stronger ocean circulation and increased melting under Pine Island Glacier ice shelf, *Nat. Geosci.*, 4, 519–523, doi:10.1038/ngeo1188.
- Jenkins, A., and S. Jacobs (2008), Circulation and melting beneath George VI Ice Shelf, Antarctica, *J. Geophys. Res.*, 113, C04013, doi:10.1029/2007JC004449.
- Joughin, I. R., R. Kwok, and M. A. Fahnestock (1998), Interferometric estimation of three-dimensional ice-flow using ascending and descending passes, *IEEE Trans. Geosci. Remote Sens.*, 36, 25–37, doi:10.1109/36.655315.
- Joughin, I., S. Tulaczyk, J. L. Bamber, D. Blankenship, J. W. Holt, T. Scambos, and D. G. Vaughan (2009), Basal conditions for Pine Island and Thwaites Glaciers, West Antarctica, determined using satellite and airborne data, *J. Glaciol.*, 55, 245–257, doi:10.3189/002214309788608705.

- Joughin, I., R. B. Alley, and D. M. Holland (2012), Ice-sheet response to oceanic forcing, *Science*, 338, 1172–1176, doi:10.1126/science.1226481.
- Joughin, I., B. E. Smith, and B. Medley (2014a), Marine ice sheet collapse potentially underway for the Thwaites Glacier basin, West Antarctica, *Science*, 344, 735–738, doi:10.1126/science.1249055.
- Joughin, I., B. Smith, D. E. Shean, and D. Floricioiu (2014b), Brief communication: Further summer speedup of Jakobshavn Isbrae, *Cryosphere*, 8, 209–214, doi:10.5194/tc-8-209-2014.
- Kimura, S., K. W. Nicholls, and E. Venables (2015), Estimation of ice shelf melt rate in the presence of a thermohaline staircase, *J. Oceanogr.*, 45, 133–148, doi:10.1175/JPO-D-13-0219.1.
- MacAyeal, D. R. (1993), A tutorial on the use of control methods in ice-sheet modeling, *J. Glaciol.*, 39, 91–98.
- McMillan, M., A. Shepherd, A. Sundal, K. Briggs, A. Muir, A. Ridout, A. Hogg, and D. Wingham (2014), Increased ice losses from Antarctica detected by CryoSat-2, *Geophys. Res. Lett.*, 41, 3899–3905, doi:10.1002/2014GL060111.
- Michel, R., and E. Rignot (1999), Flow of Glacier Moreno, Argentina, from repeat-pass Shuttle Imaging Radar images: Comparison of the phase correlation method with radar interferometry, *J. Glaciol.*, 45, 93–100.
- Moffat, C., B. Owens, and R. C. Beardsley (2009), On the characteristics of circumpolar deep water intrusions to the west Antarctic Peninsula continental shelf, *J. Geophys. Res.*, 114, C05017, doi:10.1029/2008JC004955.
- Moon, T., I. Joughin, B. Smith, M. R. van den Broeke, W. J. van de Berg, B. Noël, and M. Usher (2014), Distinct patterns of seasonal Greenland glacier velocity, *Geophys. Res. Lett.*, 41, 7209–7216, doi:10.1002/2014GL061836.
- Morlighem, M., E. Rignot, H. Seroussi, E. Larour, H. Den Bha, and D. Aubry (2010), Spatial patterns of basal drag inferred using control methods from a full-stokes and simpler models for Pine Island Glacier, West Antarctica, *Geophys. Res. Lett.*, 37, L14502, doi:10.1029/2010GL043853.
- Mouginot, J., B. Scheuchl, and E. Rignot (2012), Mapping of ice motion in Antarctica using synthetic-aperture radar data, *J. Remote Sens.*, 4(9), 2753–2767, doi:10.3390/rs4092753.
- Mouginot, J., E. Rignot, and B. Scheuchl (2014), Sustained increase in ice discharge from the Amundsen Sea Embayment, West Antarctica, from 1973 to 2013, *Geophys. Res. Lett.*, 41, 1576–1584, doi:10.1002/2013GL059069.
- Nagler, T., H. Rott, M. Hetzenecker, and J. Wuite (2015), The Sentinel-1 mission: New opportunities for ice sheet observations, *Remote Sens.*, 7, 9371–9389, doi:10.3390/rs70709371.
- Paolo, F. S., H. A. Fricker, and L. Padman (2015), Volume loss from Antarctic ice shelves is accelerating, *Science*, 348(6232), 327–331, doi:10.1126/science.aaa0940.
- Park, J. W., N. Gourmelen, A. Shepherd, S. W. Kim, D. G. Vaughan, and D. J. Wingham (2013), Sustained retreat of the Pine Island Glacier, *Geophys. Res. Lett.*, 40, 2137–2142, doi:10.1002/grl.50379.
- Payne, A. J., A. Vieli, A. P. Shepherd, D. J. Wingham, and E. Rignot (2004), Recent dramatic thinning of largest West Antarctic ice stream triggered by oceans, *Geophys. Res. Lett.*, 31, L23401, doi:10.1029/2004GL021284.
- Potter, J. R., and J. G. Paren (1985), Interaction between ice shelf and ocean in George VI Sound, Antarctica, *Antarct. Res. Ser.*, 43, 35–58, doi:10.1029/AR043p0035.
- Pritchard, H. D., S. R. M. Ligtenberg, H. A. Fricker, D. G. Vaughan, M. R. van den Broeke, and L. Padman (2012), Antarctic ice-sheet loss driven by basal melting of ice shelves, *Nature*, 484, 502–505, doi:10.1038/nature10968.
- Rignot, E. (2008), Changes in West Antarctic ice stream dynamics observed with ALOS PALSAR data, *Geophys. Res. Lett.*, 35, L12505, doi:10.1029/2008GL033365.
- Rignot, E., J. Bamber, M. van den Broeke, C. Davis, Y. Li, W. van de Berg, and E. van Meijgaard (2008), Recent Antarctic ice mass loss from radar interferometry and regional climate modelling, *Nat. Geosci.*, 1(2), 106–110, doi:10.1038/ngeo102.
- Rignot, E., J. Mouginot, and B. Scheuchl (2011a), Ice flow of the Antarctic Ice Sheet, *Science*, 333(6048), 1427–1430, doi:10.1126/science.1208336.
- Rignot, E., J. Mouginot, and B. Scheuchl (2011b), Antarctic grounding line mapping from differential satellite radar interferometry, *Geophys. Res. Lett.*, 38, L10504, doi:10.1029/2011GL047109.
- Rignot, E., J. Mouginot, M. Morlighem, H. Seroussi, and B. Scheuchl (2014), Widespread, rapid grounding line retreat of Pine Island, Thwaites, Smith and Kohler glaciers, West Antarctica, *Geophys. Res. Lett.*, 41, 3502–3509, doi:10.1002/2014GL060140.
- Rosanov, C. E., B. K. Lucchitta, and J. G. Ferrigno (1998), Velocities of Thwaites Glacier and smaller glaciers along the Marie Byrd Land coast, West Antarctica, *Ann. Glaciol.*, 27, 47–53, doi:10.3189/172756494794587573.
- Rott, H., D. Floricioiu, J. Wuite, S. Scheiblauer, T. Nagler, and M. Kern (2014), Mass changes of outlet glaciers along the Nordenskjöld Coast, northern Antarctic Peninsula, based on TanDEM-X satellite measurements, *Geophys. Res. Lett.*, 41, 8123–8129, doi:10.1002/2014GL061613.
- Scambos, T. A., C. Hulbe, M. Fahenstock, and J. Bohlander (2000), The link between climate warming and break-up of ice shelves in the Antarctic Peninsula, *J. Glaciol.*, 46(154), 516–530, doi:10.3189/172756500781833043.
- Schoof, C. (2007), Ice sheet grounding line dynamics: Steady states, stability and hysteresis, *J. Geophys. Res.*, 112, F03S28, doi:10.1029/2006JF000664.
- Scharroo, R., and P. Visser (1998), Precise orbit determination and gravity field improvement for the ERS satellites, *J. Geophys. Res.*, 103(C4), 8113–8127, doi:10.1029/97JC03179.
- Schmidtko, S., K. J. Haywood, A. F. Thompson, and A. Aoki (2014), Multidecadal warming of Antarctic waters, *Science*, 346(2614), 1227–1231, doi:10.1126/science.1256117.
- Shepherd, A., D. Wingham, J. A. D. Mansley (2002) Inland thinning of the Amundsen Sea sector, West Antarctica, *Geophys. Res. Lett.*, 29(10), 1364, doi:10.1029/2001GL014183.
- Shepherd, A., D. Wingham, T. Payne, and P. Skvarca (2003), Larsen ice shelf has progressively thinned, *Science*, 302(5646), 856–859, doi:10.1126/science.1089768.
- Shepherd, A., and D. Wingham (2007), Recent sea-level contributions of the Antarctic and Greenland Ice Sheets, *Science*, 315, 1529–1532, doi:10.1126/science.1136776.
- Shepherd, A., D. Wingham, D. Wallis, K. Giles, S. Laxon, and A. V. Sundal (2010), Recent loss of floating ice and the consequent sea level contribution, *Geophys. Res. Lett.*, 37, L13503, doi:10.1029/2010GL042496.
- Shepherd, A., et al. (2012), A reconciled estimate of ice-sheet mass balance, *Science*, 338, 1183–1189, doi:10.1126/science.1228102.
- Shuman, C. A., E. Berthier, and T. A. Scambos (2011), 2001–2009 elevation and mass losses in the Larsen A and B embayments, Antarctic Peninsula, *J. Glaciol.*, 57(204), 737–754, doi:10.3189/002214311797409811.
- Strozzi, T., A. Luckman, T. Murray, U. Wegmüller, and C. L. Werner (2002), Glacier motion estimation using SAR offset-tracking procedures, *IEEE Trans. Geosci. Remote Sens.*, 40, 2384–2391, doi:10.1109/TGRS.2002.805079.
- Talbot, M. H. (1988), Oceanic environment of George VI Ice Shelf, Antarctic Peninsula, *Ann. Glaciol.*, 11, 161–164.

- Thomas, E. R., G. J. Marshall, and J. R. McConnell (2008), A doubling in snow accumulation in the western Antarctic Peninsula since 1850, *Geophys. Res. Lett.*, *35*, L01706, doi:10.1029/2007GL032529.
- Thomas, R. H. (1984) Ice sheet margins and ice shelves, in *Climate Processes and Climate Sensitivity*, edited by J. E. Hansen and T. Takahashi, pp. 265–274, AGU, Washington, D. C., doi:10.1029/GM029p0265.
- Vaughan, D. G., and C. S. M. Doake (1996), Recent atmospheric warming and retreat of ice shelves on the Antarctic Peninsula, *Nature*, *379*, 328–331, doi:10.1038/379328a0.
- Wouters, B., J. L. Bamber, M. R. van den Broeke, J. T. M. Lenaerts, and I. Sasgen (2013), Limits in detecting acceleration of ice sheet mass loss due to climate variability, *Nat. Geosci.*, *6*, 613–616, doi:10.1038/ngeo1874.
- Wouters, B., A. Martin-Español, V. Helm, T. Flament, J. M. van Wessem, S. R. M. Ligtenberg, M. R. van den Broeke, and J. L. Bamber (2015), Dynamic thinning of glaciers on the Southern Antarctic Peninsula, *Science*, *348*, 899–903, doi:10.1126/science.aaa5727.